Bioresources Development Conference (BDC26)
NABDA
Journal of Biotechnology Research
ISSN: 1119-0531
Special Issue Vol. 5(2): (2026)

Development and Antimicrobial Performance of Chitosan-Silver Nanocomposites as Sustainable Biomaterials for Building Technology Applications

*[1]Sumaila A., [1]Yahaya, M. K., [1] Ibrahim, J., [1]Abdulazeez, M. A., [1]Ibrahim, A.,[2]Apeh, K.A., [2]Attah, F., and [3]Peter B. B.[3]

[1]Department of Chemistry, Confluence University of Science and Technology, Osara, Kogi State, Nigeria; [2]Department of Microbiology, Confluence University of Science and Technology, Osara, Kogi State, Nigeria; [3]Department of Building Construction Technology, Minna Institute of Technology and Innovation, Niger State, Nigeria

Corresponding Author: sumailaa@custech.edu.ng, +2349138281565

Article ID: NJBR-BDC26-A006 | Received: 22 July, 2025 | Accepted: 30 July, 2025

ABSTRACT

The growing demand for sustainable and eco-friendly materials has driven the development of bio-based nanocomposites with enhanced functional properties. In this study, chitosan, a naturally derived biopolymer from crustacean shells, was engaged as a matrix for the synthesis of chitosan-silver nanocomposites. The nanocomposites were biosynthesized via an in-situ reduction method, using nanosilver and the leaf extract of Nicotiana tabacum as a stabilizing and reducing agent, respectively, thereby eliminating the need for harmful chemicals. The prepared nanocomposites were characterized using Fourier Transform Infrared spectroscopy (FTIR), X-ray diffraction (XRD), and Brunauer-Emmett-Teller (BET) to confirm the functional groups, crystallinity, and surface area dispersion of silver nanoparticles (AgNPs) within the chitosan matrix. Results demonstrated the successful biosynthesis of large-surface-area silver nanoparticles with strong interactions with the chitosan backbone. The antimicrobial activity of the nanocomposites was evaluated against both Gram-positive and Gram-negative bacteria, showing significant inhibitory effects compared to pure chitosan. This work highlights the potential of utilizing bioresources in the development of functional nanocomposites for biomedical and environmental applications, contributing to the advancement of sustainable nanotechnology.

Key words: Antimicrobial, Biopolymer, Crustacean Shells, Eco-friendly Materials, Nanocomposites

INTRODUCTION

The escalating challenges of antibiotic resistance and environmental pollution necessitate the development of innovative materials that are both effective and sustainable (Hossein and Ripanda, 2025). Chitosan, a biopolymer derived from chitin found in crustacean exoskeletons, has garnered significant attention due to its biodegradability, biocompatibility, and inherent antimicrobial properties (Hisham *et al.*, 2023). When combined with silver nanoparticles (AgNPs), known for their potent antimicrobial activity, chitosan forms nanocomposites that exhibit enhanced functionalities suitable for various applications, including biomedical devices, water purification systems, and food packaging (Charti *et al.*, 2025).

The synthesis of chitosan-silver nanocomposites can be achieved through various methods, including chemical reduction, green synthesis, and physical approaches. Chemical reduction methods often involve the use of reducing agents to convert silver ions into metallic silver, which is then incorporated into the chitosan matrix (Shayo, Elimbinzi, and Shao, 2024). For instance, a study by Zaidi *et al.* (2023) reported the synthesis of chitosan-silver nanocomposites using a chemical reduction method, followed by characterization techniques such as UV-Vis spectroscopy and scanning electron microscopy (SEM) to confirm the formation and morphology of the nanocomposites. Green synthesis methods, on the other hand, utilize natural reducing agents, offering an eco-friendly alternative to traditional chemical processes (Abady *et al.*, 2025). For example, a study by Rajabloo *et al.* (2022) demonstrated the green synthesis of chitosan-silver nanocomposites reinforced with curcumin nanoparticles, highlighting their enhanced antibacterial properties.

The characterization of these nanocomposites is crucial to understanding their structural, chemical, and physical properties. Techniques such as Fourier-transform infrared (FTIR) spectroscopy, X-ray

diffraction (XRD), and Brunauer, Emmett, and Teller (BET) are commonly employed to analyze the functional groups, crystallinity, and surface area of the nanocomposites (Ali *et al.*, 2023). For instance, X-ray Photoelectron Spectroscopy (XPS) analysis has been used to determine the valence states of silver in chitosan-silver nanocomposite films, confirming the presence of metallic silver and the successful reduction of silver ions (Laanoja *et al.*, 2024).

The antimicrobial efficacy of chitosan-silver nanocomposites has been extensively studied, with promising results against a wide range of pathogens, including bacteria and fungi (Dhlamini *et al.,* 2024; Nasaj *et al.*, 2024; Safari *et al.*, 2024). The incorporation of silver nanoparticles into the chitosan matrix enhances its antimicrobial activity, making it a potential candidate for applications in wound dressings, medical devices, and food preservation. Moreover, the biocompatibility of chitosan ensures that these nanocomposites are safe for use in biomedical applications (Yao *et al.*, 2025).

This research aims to prepare and characterize chitosan-silver nanocomposites, exploring their potential for sustainable bioresource utilization and antimicrobial applications. By leveraging the natural abundance of chitosan and the antimicrobial properties of silver, this study seeks to contribute to the development of eco-friendly materials that address pressing global challenges.

MATERIALS AND METHODS

Materials

This study used crab shells and *Nicotiana tabacum* leaves obtained from a local fish market in New Bussa and Tunga Awuje village, Niger State, Nigeria, respectively. The crab shells were washed, air-dried for two weeks, and pulverized before being filtered into fine particles for extraction. The leaves were washed, distilled, air-dried, and milled into powder before being stored for further analysis.

Methods

The production of chitosan from the powdered crab shells involved deproteinization, demineralization, and deacetylation.

Deproteinization of the Crab Shells: To deproteinize the Crab Shells, 5 g of the crab shells were put into a 250 cm^3 beaker, treated with 1.25 M NaOH at 30 ^{0}C for three hours. After heating, the mixtures were allowed to cool and settle; excess NaOH was removed by decantation, followed by washing with deionized water to neutral pH. Filtration was done using Whatman filter paper No 4; the residue was oven-dried at 80 ^{0}C for 45 minutes (Sumaila *et al.*, 2020).

Demineralization of the Deproteinized Crab Shells: For the demineralization of the Deproteinized Crab Shells, 3 g of the deproteinized crab shells were inserted into a 250 cm^3 conical flask, treated with 1.25 M HCl at 80 ^{0}C for five hours. Subsequently, the mixture was allowed to cool and settle; excess HCl was removed by decantation, followed by washing with deionized water to neutral pH. This was later followed by filtration using Whatman filter paper No 4, and the residue (chitin) obtained was oven-dried at 80 ^{0}C for 45 minutes.

Deacetylation of Chitin: In order to deacetylate the obtained chitin, 1 g of the chitin was put in 100 cm^3 beakers, treated with 0.5 M NaOH at 100^{0}C for two hours. Subsequently, the mixture was allowed to cool and settle; excess NaOH was removed by decantation, followed by washing with deionized water to neutral pH. Thereafter, filtration was done using Whatman filter paper No 4, and the residue (chitosan) was oven-dried at 80 ^{0}C for 45 minutes.

Determination of Moisture Content: The determination of the moisture content of the produced chitosan was carried out by weighing 0.5 g of the chitosan into a porcelain crucible, heating it in an oven at 60^{0}C for 1 hour, and reweighing after cooling until a constant weight was obtained (Sumaila *et al.*, 2020). The moisture content was then calculated using Equation 1.

$$\% \text{ Moisture content} = \frac{W_b - W_a}{W_b} \text{x } 100\% \quad (1)$$

w_b = Weight of chitosan before heating, and w_a = Weight of chitosan after heating.

Determination of Ash Content: To determine the ash content of the prepared chitosan, 2 g of the chitosan sample was placed into a crucible and heated in a furnace to 550 ^{0}C for 2 hours. The sample

was allowed to cool, and the weight of the ash residue was measured, and the empty crucible was weighed separately (Sumaila *et al*., 2020). Equation 2 was employed to calculate the ash content.

$$\text{Ash Content \%} = \frac{\text{Weight of the ash residue (g)}}{\text{Weight of the sample (g)}} \times 100$$

Preparation of the Aqueous Leaf Extract of *Nicotiana tabacum:* To prepare the Aqueous Leaf Extract of *Nicotiana tabacum*, 1 g of the powdered *Nicotiana tabacum* leaves were put in a 250 cm^3 beaker, followed by the addition of 100 cm^3 distilled water. The mixture was shaken and heated at 80 °C in a water bath for 15 minutes. This was allowed to cool and subsequently filtered using Whatman No.1 filter paper and stored at room temperature for further use (Ileke, Idoko, Ojo, and Adesina, 2020).

Preparation of Chitosan - Silver Nanocomposite: The preparation of chitosan-silver nanocomposites (COMP 1:1, COMP 1:2, and COMP 2:1) was done by varying the amounts of acetic acid solutions of chitosan and aqueous solutions of silver nitrate, as shown in Table 1(Wahab *et al*., 2023). Nanocomposite (COMP 1:1) was prepared by the addition of 5 cm^3 aqueous leaf extract of *Nicotiana tabacum* to the mixture of 40 cm^3 of 1% chitosan and 40 cm^3 of 1 mM silver nitrate solutions, and stirred on a magnetic stirrer at 250 rpm for 2 hours, and subsequently allowed to age for 24 hours. The obtained chitosan-silver nanocomposite film was freeze-dried at -42 °C and then stored for characterization. The other experimental runs to prepare nanocomposites (COMP 1:2 and COMP 2:1) were carried out using the conditions set out in Table 1 (Sumaila *et al*., 2020).

Table 1: Experimental Runs for the Preparation of Chitosan-Silver Nanocomposites

Run	Amount of Chitosan (wt %)	Amount of silver nitrate (mM)	Sample
1	1.00	1.00	COMP 1:1
2	1.00	2.00	COMP 1:2
3	2.00	1.00	COMP 2:1

Characterization of the Prepared Chitosan, Nanosilver, and Chitosan-Silver Nanocomposite: The prepared chitosan, silver nanoparticles, and chitosan-silver nanocomposites (COMP 1:1, COMP1:2, and COMP 2:1) were characterized by determining their specific surface areas, mineralogical phases, and functional groups by BET, XRD, and FTIR.

Determination of the Antibacterial Activities of Chitosan, Silver Nanoparticles and Chitosan-Silver Nanocomposites: The antimicrobial activities of the chitosan, nanosilver, and chitosan-silver nanocomposites (COMP 1:1, COMP 1:2, and COMP 2:1) against *B. Megaterium, E. Coli, S.typhi, K. pneumoniae, P. aeruginosa, S. aureus, and S. pyogimase* were determined using the agar well diffusion bioassay. The microbial cultures were procured from the Department of Microbiology, Federal University of Technology, Minna, Niger State.

Individually, a single colony of bacterial strain was grown in nutrient broth and maintained on a shaker at 37 °C for 24 hours. After 24 hours, the bacterial cultures were uniformly spread on Mueller-Hinton plates. Wells of 10 mm diameter each were made using a sterilized gel borer. Each well was filled with 5mg/cm^3 solution of chitosan, nanosilver, and chitosan-silver nanocomposites (COMP 1:1, COMP 1:2, and COMP 2:1), respectively. The test samples were incubated at 37°C for 24 hours, then the zones of inhibition were measured in mm using a measuring scale (Festus and Emmanuella, 2020).

Statistical Analysis

All experimental data were analyzed using descriptive statistics. Measurements of inhibition zones were expressed as the mean from at least three independent replicates. Additionally, correlation analysis was conducted to assess the relationship between chitosan and silver nanoparticles in terms of their antimicrobial activity. The strength and direction of these associations were interpreted using Pearson's correlation coefficient (r).

RESULTS AND DISCUSSION

Determination of Moisture and Ash Contents of the Prepared Chitosan

The results from Table 2 reveal that the chitosan obtained in this study had moisture and ash contents

of 2.94 and 6.25 %, respectively. The moisture content of the chitosan was measured at 2.94%, lower than the 9.34% reported by Puvvada *et al.* (2012). Good-quality chitosan should have a moisture content of less than 10% after adequate deproteination, demineralization, and deacetylation processes. The ash content was 6.25%, close to 6.41% reported by Isa *et al.* (2012) but lower than the 36.87% reported by Abdulkarim *et al.* (2013) for chitosan samples from Nigerian shrimp and mussel shell. This value is close to the 5% ash content recommended for high-quality chitosan.

Table 2: Results of physicochemical properties of the Produced Chitosan

Properties	Value (%)
Moisture Content	2.94
Ash Content	6.25

Results of the Phytochemical Screening of Aqueous Leaf Extract of *Nicotiana tabacum*

This study identified and determined the amount of phytochemicals in the aqueous leaf extract of *Nicotiana tabacum* and revealed the presence of alkaloids, flavonoids, phenols, and tannins (Table 3**),** which are crucial for the biosynthesis of metal nanomaterials. The quantitative phytochemical analysis of *Nicotiana tabacum* leaf extracts (Table 3**)** shows a high concentration of total phenols (135.41 mg/g), alkaloids (72.722 mg/g), tannins (45.70 mg/g), and flavonoids (23.67 mg/g). These findings align with previous studies by Okere *et al.* (2016), Sunil *et al.* (2010), and Oyekunle *et al.* (2019), suggesting their potential for silver nanoparticle biosynthesis. Thus, there is a need to explore plants with these reducing values for metal nanomaterial preparation.

Table 3: Qualitative and Quantitative Phytochemical Analysis of Aqueous Leaf Extracts of *Nicotiana tabacum* (mg/g)

Compounds	Aqueous extracts	Amount (mg/g)
Total Alkaloids	+	72.72
Total Phenols	+	135.41
Total Flavonoids	+	23.67
Tannins	+	45.70
Reducing sugars	-	-
Saponins	-	-

Key: Positive (+), Negative (-)

Results of Characterization of Chitosan, Silver Nanoparticles, and Chitosan-Silver Nanocomposites

Fourier transmission infrared (FTIR) spectra of chitosan, silver nanoparticles, and chitosan – silver nanocomposites: FTIR spectroscopy is crucial for characterizing nanomaterial surface chemistry, revealing organic functional groups. This study obtained FTIR spectra (Figure 1) of chitosan, silver nanoparticles, and chitosan-silver nanocomposites (COMP 1:1, COMP 1:2, and COMP 2:1).

The FTIR spectrum of chitosan and silver nanoparticles reveals peaks at 3304.74, 2872.84, 1660.75, 1409.97, 1033.81, 866.62, and 713.37 cm^{-1}. These peaks are attributed to the overlapping peaks of the N-H and O-H stretching vibrations. The absorption peaks at 3304.74 cm^{-1} are attributed to the N-H and O-H stretching vibrations (Hansen *et al.*, 2021). The absorbance peaks at 2872.84, 1660.75, and 1409.97 cm^{-1} indicate the presence of C-H stretching of polymeric link, N-H in-plane bend, and O- H in-plane deformation, respectively. The characteristic absorption peaks at 1033.81 and 866.62 cm^{-1} are attributed to C-O stretching of O-H groups due to deformation. The FTIR spectrum of the silver nanoparticles reveals the likely biomolecules present in the leaf extract that aided the reduction of silver ions into silver nanoparticles. The FTIR spectra of the chitosan-silver nanocomposites show similar surface functional groups to chitosan but varied absorption intensities and frequencies of O-H deformation in-plane and N-H in-plane bending. The FTIR spectra agree with the results reported by An *et al.* (2011) for chitosan nanocomposite.

Brunauer-Emmett Teller (BET) Surface area, pore size, and pore volume of chitosan, silver nanoparticles, chitosan-silver nanocomposites: The BET method was used to analyze the surface area, pore sizes, and pore volumes of extracted chitosan, biosynthesized silver nanoparticles, and chitosan-silver nanocomposites. The results (Table 4) showed specific surface areas of 12.67,

139.20, 26.07, 38.20, and 33.46 m^2/g for chitosan, silver nanoparticles, and chitosan-silver nanocomposites, respectively.

The study measured the BET surface areas of chitosan, silver nanoparticles, and chitosan-silver nanocomposites using the N_2 adsorption isotherm. The surface area of chitosan increased to 26.07, 38.20, and 33.46 m^2/g for composites of chitosan-silver, with a specific surface area of silver nanoparticles of 139.20 m^2/g. This increase may be due to the reduction of agglomeration caused by the presence of silver nanoparticles in the polymer matrix of chitosan (Wahab *et al*., 2023). The composite of chitosan with silver nanoparticles will show better potential for adsorption compared to chitosan. The pore volume (Table 4) of the prepared chitosan increased from 0.0266 cm^3/g to 0.1152, 0.1430, and 0.1347 cm^3/g for the composites loaded with nanosilver. This finding is similar to those of chitosan nanofibers functionalized by TiO_2 nanoparticles for antimicrobial wound healing applications (Nosrati and Heydari, 2025).

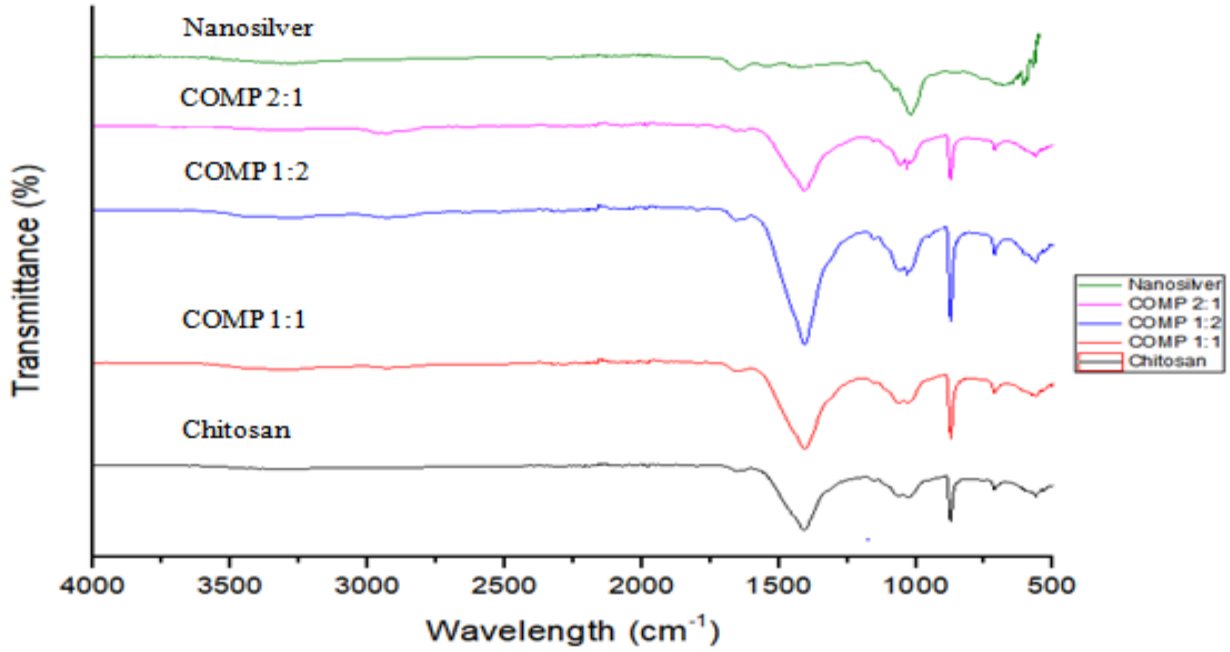


Figure 1: FTIR spectrum of chitosan, silver nanoparticles and chitosan-silver nanocomposites (COMP 1:1, COMP 1:2, and COMP 2:1)

Table 4 shows the mean pore sizes of the prepared chitosan, nanosilver and nanocomposites, while Figure 2 shows that, based on the pore size distribution, chitosan, silver nanoparticles, and chitosan-silver nanocomposites were all mesoporous in nature. Meanwhile, according to the International Union of Pure and Applied Chemistry (IUPAC), pores are classified on the basis of diameter [macropores (d>50 nm), mesopores (2<d<50 nm), and micropores (d<2 nm)].

Figure 3 shows that chitosan, nanosilver, and their nanocomposites exhibited a Type III adsorption isotherm, which explains the formation of multilayer materials (Sapna and Dinesh, 2019).

Table 4: Results of BET Analysis of Chitosan, Silver Nanoparticles, and Chitosan-Silver Nanocomposites (COMP 1:1, COMP 1:2, and COMP 2:1)

S/N	Material	Specific Surface area (m^2/g)	Mean Pore volume (cm^3/g)	Mean Pore size (nm)
1	Chitosan	12.67	0.0266	4.035
2	Nanosilver	139.20	0.2087	3.599
3	COMP 1:1	26.07	0.1152	4.068
4	COMP 1:2	38.20	0.1430	4.080
5	COMP 2:1	33.46	0.1347	4.078

NABDA
Journal of Biotechnology Research
ISSN: 1119-0531
Special Issue Vol. 5(2): (2026)

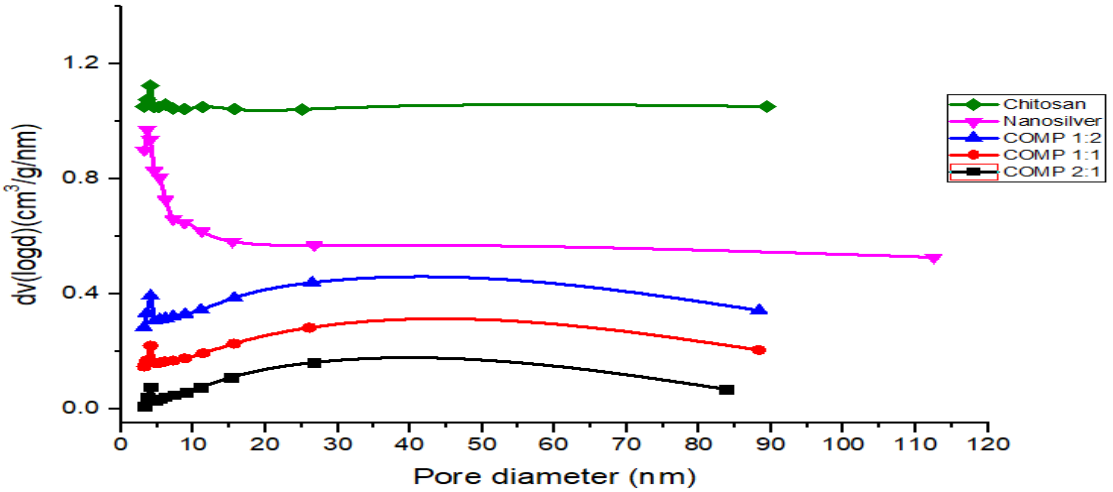


Figure 2: Pore size distributions of the extracted chitosan, biosynthesized silver nanoparticles and chitosan-silver nanocomposites (COMP 1:1, COMP 1:2, and COMP 2:1)

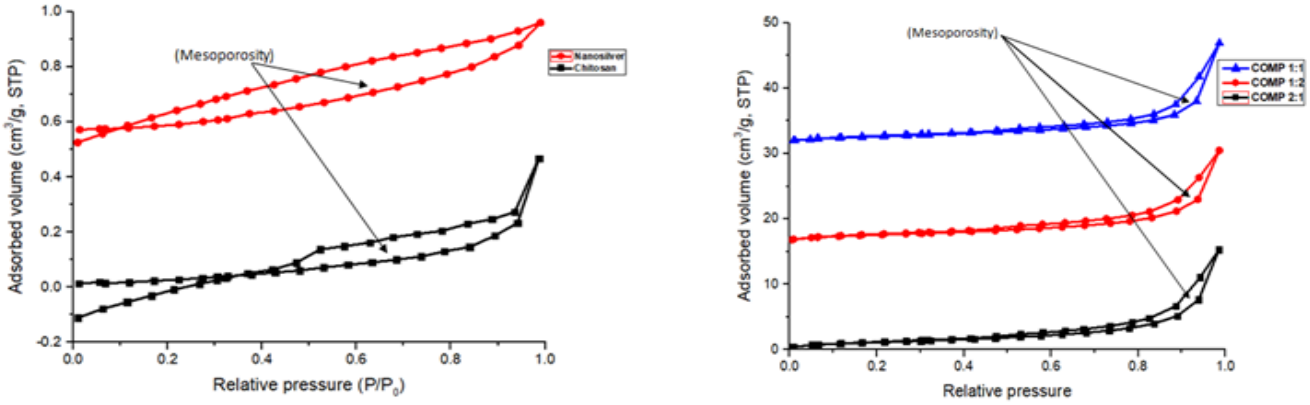


Figure 3: Isotherm types of the extracted chitosan; nanosilver and chitosan-silver nanocomposites (COMP 1:1, COMP 1:2, and COMP 2:1)

X-Ray Diffraction (XRD) pattern of the prepared chitosan, silver nanoparticles, and chitosan-silver nanocomposites (COMP 1:1, COMP 1:2, and COMP 2:1): The phase structures of the prepared chitosan, silver nanoparticles, and chitosan-silver nanocomposites (COMP 1:1, COMP 1:2, and COMP 2:1) were investigated using the XRD technique. The diffraction angles were taken for the 2θ range of 0 to 75 degrees. The peaks positioning the unit cell dimensions, known as indexing, were determined as the primary step in the diffraction pattern analysis. Miller indices (h, k, and l) were assigned for each peak to index. The X-ray diffraction patterns of the samples are shown in Figure 4. The XRD pattern of chitosan revealed two main diffraction peaks at 2θ of 12.56° and 19.30°, corresponding to planes (020) and (110) typical of semi-crystalline chitosan (Sumaila *et al.*, 2020). These peaks could be related to crystal I and II in the chitosan structure and attributable to the high degree of crystallinity of the prepared chitosan (Podgorbunskikh *et al.*, 2022). The crystallinity of chitosan is 69.54%, while the XRD pattern of silver nanoparticles shows three typical peaks at 2θ values of 38.15, 44.26, and 64.650 corresponding to (111), (200), and (220) planes of nanosilver. These values compared well with those of the standard powder diffraction card of JCPDS, silver file No. 04-0783. The XRD study confirms that the resultant particles are face-centered cubic (FCC) silver nanoparticles, formed by the reduction of Ag^+ ions by the *Nicotiana tabacum* leaves extract. A peak at 2θ of 38.150 signifies a smaller particle size of the nanoparticles, while additional peaks not indexed in the diffractogram are probably due to the remnant biomolecules of the leaf extract.

The X-ray diffraction (XRD) patterns of the chitosan-silver nanocomposites (COMP 1:1, COMP 1:2, and COMP 2:1) were compared to the chitosan polymer matrix to reveal the effect of the silver nanoparticle loads on the chitosan polymer structure. The XRD patterns displayed signals at 2θ of 9.29 and 19.30°, 38.04, 44.65, and 64.45° characteristic of the planes (020) and (110), (111), (200),

and (220) of chitosan and the FCC structure of Ag. No diffraction peaks corresponding to Ag_2O were observed in the XRD patterns of the nanocomposites and nanosilver, indicating no oxidation of the silver nanoparticles during the preparation of the nanocomposites (Akhter *et al.*, 2024). The presence of unassigned diffraction peaks could be attributed to the biomolecules of the leaf extract used in the preparation of the nanocomposites (Mulu*et al.*, 2024). The XRD pattern of chitosan showed two typical peaks at 2θ =12.56° and 19.30°, but due to the interaction of Ag^+ ions, the peak at 12.560 of chitosan shifted to 9.30° while the peak at 19.30 remained unchanged. As the amount of silver nanoparticles in the nanocomposites increased, the diffraction peaks increased in intensity, resulting in decreased and increased intensities of the crystalline and amorphous zones of the polymer, respectively.

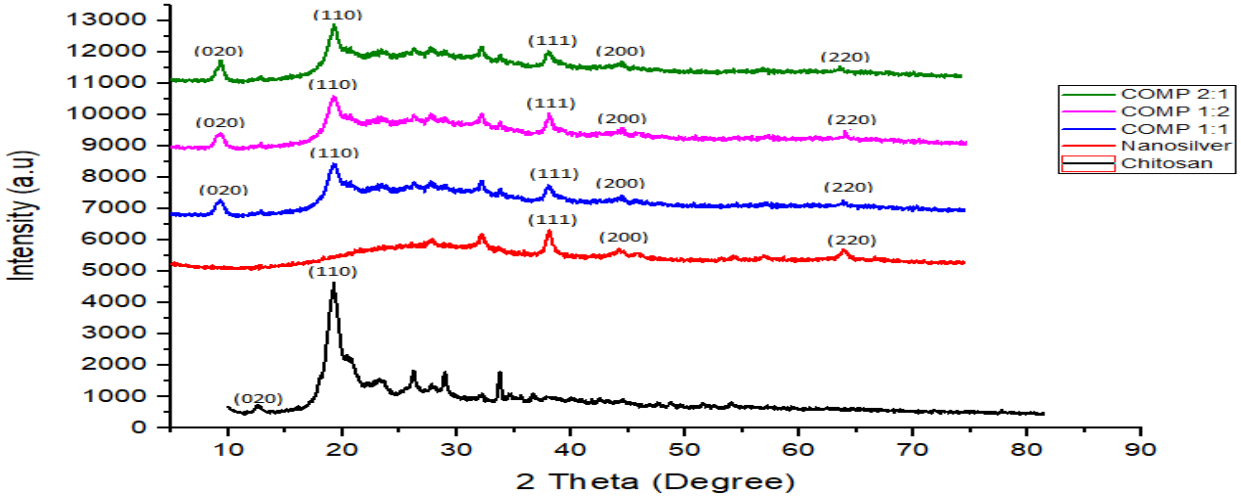


Figure 4: XRD patterns of the prepared chitosan, silver nanoparticles, and chitosan-silver nanocomposites (COMP 1:1, COMP 1:2, and COMP 2:1)

Results of Antimicrobial Activities of Chitosan and its Silver Nanocomposites

In this work, the antimicrobial potentials of the prepared chitosan-silver nanocomposites (COMP 1:1, COMP 1:2, and COMP 2:1) were assessed against seven selected bacterial strains (*Bacillus megaterium, Escherichia coli, Klebsciella pneumaniae, P. aeruginosa, S. typhi, S. pyroginase and S. aureus*) consisting of four Gram-negative and three-gram positive bacteria strains by the agar diffusion method, using chitosan and silver nanoparticles as controls. The results of the antimicrobial studies are shown in Figure 5. The study found that chitosan and silver nanoparticles had less inhibitory activity against test organisms than chitosan-silver nanocomposites. Chitosan showed zones of inhibition against *S. aureus* and *P. aeruginosa*, but no zones were observed against *B. megaterium, E.coli, K. pneumaniae, S. typhi*, and *S. pyroginase*. The true mechanisms of chitosan's inhibition are not yet fully understood, but it is associated with changes in cell permeability due to interactions between chitosan and microorganism cell membranes (Doan *et al.*, 2025).

The study shows that silver nanoparticles exhibit the highest zone of inhibition against S*. typhi,* with a zone of inhibition of 35 mm. Silver nanoparticles are known for their antibacterial activity against various Gram-positive and Gram-negative bacteria (Torrens and Cava, 2024). The antimicrobial activity of chitosan improved significantly after incorporating nanosilver to form chitosan-silver nanocomposites, possibly due to increased dispersion and surface area. The inhibition strengths of chitosan, nanosilver, and chitosan-silver nanocomposites were more significant on Gram-negative bacteria than Gram-positive ones, but were efficient in both cases. This could be attributed to the hydrophilicity of cell walls and negatively charged cell surfaces in Gram-negative bacteria (Akdaşçi *et al.*, 2025).

The zones of inhibition were directly proportional to the amounts of both chitosan and nanosilver. The high zones of inhibition on Gram-negative bacteria may be due to their thin cell wall and negative electrostatic charges, which facilitate easy diffusion of samples (Zhydzetski *et al.*, 2024). The study found that COMP 1:2 was the most effective against bacteria due to the higher amount and larger dispersion of nanosilver on its surface. *S. typhi* maintained inhibition of not less than 30 mm for all

samples, except for chitosan, which had no clear inhibition. The least inhibited microorganism was *P. aeruginosa,* with a zone of inhibition of about 20 mm.

Using regression statistical analysis (Table 5) and employing the inhibition zone as the response variable, it was observed that for all the tested bacteria, the coefficients of correlation (R^2) were positive, suggesting that the inhibitory effects of nanocomposites were directly proportional to the ratio of chitosan to nanosilver in the nanocomposites.

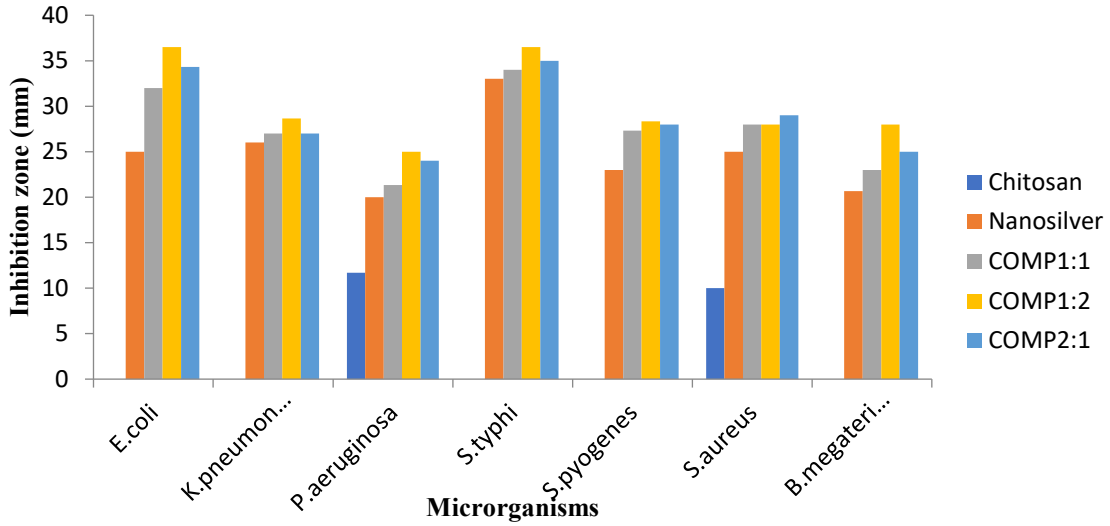


Figure 5: Results of antimicrobial activities of chitosan, silver nanoparticles and chitosan-silver nanocomposites

Table 5: Correlation of Zones of Inhibition and Concentrations of Silver Nanoparticles and Chitosan

	Correlation Coefficients (R)	
Bacteria	**Silver nanoparticles**	**Chitosan**
Gram-negative		
E. coli	0.917	0.961
K. pneumonia	0.891	0.866
S. typhi	0.895	0.999
P. aeruginosa	0.968	0.982
Gram-positive		
B. megaterium	0.938	0.932
S. pyogimase	0.881	0.921
S. aureus	0.914	0.961

CONCLUSION AND RECOMMENDATIONS

Chitosan-silver nanocomposites have shown potential in sustainable bioresource utilization and antimicrobial applications. The preparation, characterization and application of chitosan and chitosan-silver nanocomposites were the major concerns of this study. Chitosan was obtained from crab shells via treatment using NaOH and HCl, while the green preparation of chitosan-silver nanocomposite was achieved using silver nitrate as the precursor and aqueous leaf extract of *Nicotiana tabacum* as the reducing agent. As part of this study, chitosan and its silver nanocomposites were examined for their antimicrobial activities. From the major findings of this study, the conclusions drawn were that:

i. The preparation of chitosan from crab shells was achieved
ii. Physicochemical properties revealed that the prepared chitosan had moisture content and ash content and degree to be 2.94 and 6.25%, respectively
iii. The various characterizations done revealed improvement in the quality of chitosan after incorporation of nanosilver. The FTIR results showed that chitosan and its composite with silver had surface functional groups (-OH and $-NH_2$) which could act as binding sites.

iv. XRD analysis of chitosan and its composites showed diffraction peaks at 2-theta angles corresponding to crystal planes of chitosan and nanosilver.
v. BET results showed that chitosan had its surface area increased after incorporation of silver nanoparticles.
vi. The antimicrobial activity of chitosan against the selected bacteria improved after incorporation of silver nanoparticles. Thus, chitosan and chitosan-silver nanocomposites may be used as eco-friendly adsorbents and antimicrobial agents.

Based on the conclusions drawn in this study, the following recommendations are made:

i. More plant extracts and nanoparticles of other metals should be tested for their possibility of being used as reducing agents and stabilizers for the preparation of chitosan-metal nanocomposites, respectively.
ii. Further study should be done to evaluate the potential of the prepared chitosan and chitosan-silver nanocomposites for the removal of other pollutants from aqueous and other media.
iii. Standardized protocols for synthesis, characterization, and application will facilitate regulatory approval and promote commercial adoption.
iv. Collaborations between researchers, industry stakeholders, and regulatory bodies should translate laboratory-scale findings into commercially viable products like antimicrobial coatings, wound dressings, and food packaging materials.

The results derived from this study have contributed to filling the following knowledge gaps

i. The preparation of chitosan-silver nanocomposite via simple and eco-friendly means.
ii. The instability of chitosan can be controlled using nanosilver without significant changes in the structural system of the biopolymer.
iii. The improvement of the antimicrobial potential of chitosan by stabilizing using silver nanoparticles.

REFERENCES

1. Abady, M. M., Mohammed, D. M., Soliman, T. N., Shalaby, R. A., & Sakr, F. A. (2025). Sustainable synthesis of nanomaterials using different renewable sources. *Bulletin of the National Research Centre/Bulletin of the National Research Center*, *49*(1). https://doi.org/10.1186/s42269-025-01316-4.
2. Abdulkarim, A., Isa, M. T, Abdulsalam, S., Muhammad, A. J., &Ameh, A. O. (2013). Extraction and Characterisation of Chitin and Chitosan from Mussel Shell. *Civil and Environmental Research*, *3*, (2), 108.
3. Akdaşçi, E., Duman, H., Eker, F., Bechelany, M., &Karav, S. (2025). Chitosan and its nanoparticles: a multifaceted approach to antibacterial applications. *Nanomaterials*, *15*(2), 126. https://doi.org/10.3390/nano15020126.
4. Akhter, M. S., Rahman, M. A., Ripon, R. K., Mubarak, M., Akter, M., Mahbub, S., Mamun, F. A., &Sikder, M. T. (2024). A Systematic Review on Green Synthesis of Silver Nanoparticles Using Plant Extracts and Their Bio-medical Applications. *Heliyon*, *10*(11), e29766. https://doi.org/10.1016/j.heliyon.2024.e29766.
5. Ali, M. H., Azad, M. a. K., Khan, K. A., Rahman, M. O., Chakma, U., & Kumer, A. (2023). Analysis of crystallographic structures and properties of silver nanoparticles synthesized using PKL extract and nanoscale characterization techniques. *ACS Omega*, *8*(31), 28133-28142. https://doi.org/10.1021/acsomega.3c01261.
6. An, J., Luo, Q., Yuan, X., Wang, D., & Li, X. (2011). Preparation and characterization of silver-chitosan nanocomposite particles with antimicrobial activity. *Journal of Applied Polymer Science*, *120*(6), 3180-3189. https://doi.org/10.1002/app.33532.
7. Charti, I., Sair, S., Rafik, O., Abboud, Y., & Bouari, A. E. (2025). Eco-friendly synthesis of cellulose-silver nanocomposites and the evaluation of their antibacterial activity. *Discover Nano*, *20*(1). https://doi.org/10.1186/s11671-024-04156-9.
8. Dhlamini, K. S., Selepe, C. T., Ramalapa, B., Tshweu, L., & Ray, S. S. (2024). Reimagining Chitosan-Based antimicrobial biomaterials to mitigate antibiotic resistance and Alleviate Antibiotic Overuse: a review. *Macromolecular Materials and Engineering*, *309*(9). https://doi.org/10.1002/mame.202400018.

9. Doan, N. T., Van Quan, N., Anh, L. H., Duc, N. D., &Xuan, T. D. (2025). Exploring the potential of Chitosan-Phytochemical composites in preventing the contamination of Antibiotic-Resistant bacteria on food surfaces: a review. *Molecules*, *30*(3), 455. https://doi.org/10.3390/molecules30030455.
10. Festus, N. O. D., &Emmanuella, N. O. O. (2020). Testing the efficacy of Mueller-Hinton agar over Nutrient agar for optimal antibiotic sensitivity testing response by selected clinical bacterial pathogens. *GSC Advanced Research and Reviews*, *5*(2), 061-074. https://doi.org/10.30574/gscarr.2020.5.2.0037.
11. Hansen, P. E., Vakili, M., Kamounah, F. S., &Spanget-Larsen, J. (2021). NH Stretching Frequencies of Intramolecularly Hydrogen-Bonded Systems: An Experimental and Theoretical Study. *Molecules*, *26*(24), 7651. https://doi.org/10.3390/molecules26247651.
12. Hisham, F., Akmal, M. M., Ahmad, F., Ahmad, K., & Samat, N. (2023). Biopolymer chitosan: Potential sources, extraction methods, and emerging applications. *Ain Shams Engineering Journal*, *15*(2), 102424. https://doi.org/10.1016/j.asej.2023.102424.
13. Hossein, M., & Ripanda, A. S. (2025). Pollution by antimicrobials and antibiotic resistance genes in East Africa: occurrence, sources, and potential environmental implications. *Toxicology Reports*, *14*, 101969. https://doi.org/10.1016/j.toxrep.2025.101969.
14. Ileke, K. D., Idoko, J. E., Ojo, D. O., & Adesina, B. C. (2020). Evaluation of botanical powders and extracts from Nigerian plants as protectants of maize grains against maize weevil, *Sitophilus zeamais* (Motschulsky) [Coleoptera: Curculionidae]. *Biocatalysis and agricultural biotechnology*, *27*, 101702. https://doi.org/10.1016/j.bcab.2020.101702.
15. Isa, M., Ameh, A., Tijjani, M., &Adama, K. (2012). Extraction and characterization of chitin and chitosan from Nigerian shrimps. *International Journal of Biological and Chemical Sciences*, *6*(1). https://doi.org/10.4314/ijbcs.v6i1.40.
16. Laanoja, J., Sihtmäe, M., Vihodceva, S., Iesalnieks, M., Otsus, M., Kurvet, I., Kahru, A., & Kasemets, K. (2024). Synthesis and synergistic antibacterial efficiency of chitosan-copper oxide nanocomposites. *Heliyon*, *10*(15), e35588. https://doi.org/10.1016/j.heliyon.2024.e35588.
17. Mulu, M., Tefera, M., Guadie, A., &Basavaiah, K. (2024). Biosynthesis, characterization, and study of the application of silver nanoparticles for 4-nitrophenol reduction, and antimicrobial activities. *Biotechnology Reports*, *42*, e00838. https://doi.org/10.1016/j.btre.2024.e00838.
18. Nasaj, M., Chehelgerdi, M., Asghari, B., Ahmadieh-Yazdi, A., Asgari, M., Kabiri-Samani, S., Sharifi, E., & Arabestani, M. (2024). Factors influencing the antimicrobial mechanism of chitosan action and its derivatives: A review. *International Journal of Biological Macromolecules*, *277*, 134321. https://doi.org/10.1016/j.ijbiomac.2024.134321.
19. Nosrati, H., &Heydari, M. (2025). Titanium dioxide nanoparticles: a promising candidate for wound healing applications. *Burns & Trauma*, *13*. https://doi.org/10.1093/burnst/tkae069.
20. Okere, O. S., Ejike, U. D., Mubarak, L. L., & Paul, J. (2016). Phytochemical Screening of Tobacco (*Nicotiana tabacum*) and Its Effects on Some Haematological Parameters and Histopathology of Liver and Brain in Male Rats. *International Journal of Biochemistry Research and Review 14* (4), 1-9.
21. Oyekunle, I. P., Nwogu, U., Orababa, O., Nsude, C. C., Ikpa, J. O., &Azuka, D. C. (2019). Phytochemical, Antimicrobial, and Proximate Composition of *Nicotiana tabacum Leaves* Extract. *International Journal of Innovative Science and Research Technology, 4* (5), 406-410.
22. Podgorbunskikh, E., Kuskov, T., Rychkov, D., Lomovskii, O., &Bychkov, A. (2022). Mechanical Amorphization of Chitosan with Different Molecular Weights. *Polymers*, *14*(20), 4438. https://doi.org/10.3390/polym14204438.
23. Puvvada, Y. S., Vankayalapati, S., &Sukhavasi, S. (2012). Extraction of Chitin from Chitosan Exoskeleton of Shrimp for Application in the Pharmaceutical Industry. *International Current Pharmaceutical Journal*, *1* (9), 258-263.
24. Rajabloo, Z., MobarakQamsari, E., KasraKermanshahi, R., &Farzaneh, F. (2022). Green synthesis of chitosan-silver nanocomposite reinforced with curcumin nanoparticles: characterization and antibacterial effect. *Polymer Bulletin*, 80, 5333-5352. https://doi.org/10.1007/s00289-022-04270-7
25. Safari, S., Barani, M., & Sadrmohammadi, R. (2024). "Antimicrobial properties of tissue conditioner modified with chitosan and green-synthesized silver nanoparticles: a promising approach for preventing denture stomatitis". *BMC oral health*, *24*(1), 146. https://doi.org/10.1186/s12903-024-03880-z.

26. Sapna, R., & Dinesh, K. (2019). Comparative Kinetics and Thermodynamic Studies of Fluoride Adsorption by Two Novel Synthesized Biopolymer Composites. *Carbohydrate Polymers*, *203* (1), 430-440.
27. Shayo, G. M., Elimbinzi, E., & Shao, G. N. (2024). Preparation methods, applications, toxicity, and mechanisms of silver nanoparticles as a bactericidal agent, and the superiority of the green synthesis method. *Heliyon*, *10*(17), e36539. https://doi.org/10.1016/j.heliyon.2024.e36539.
28. Sumaila, A., Ndamitso, M. M., Iyaka, Y. A., Abdulkareem, A. S., &Tijani, J. O. (2020). The Role of Chitosan (CHS) and Chitosan-Silver Nanoadsorbents (COMP) in Adsorption of Cu (II) and Fe (II) Ions from Electroplating Wastewater. *Advances in Environmental Studies*, *4*(2). https://doi.org/10.36959/742/228.
29. Sunil, K., Sharma, P., Jain, A., &Sikarwar, M. (2010). Preliminary Phytochemical Screening and HPTLC Fingerprinting of *Nicotiana tabacum* leaf. *Journal of Pharmacy Research*. 3. 1144-1145.
30. Torrens, G., & Cava, F. (2024). Mechanisms conferring bacterial cell wall variability and adaptivity. *Biochemical Society Transactions*. https://doi.org/10.1042/bst20230027.
31. Wahab, S., Ali, H. M., Khan, M., Khan, T., Krishnaraj, C., & Yun, S. (2023). Green synthesis and antibacterial assessment of chitosan/silver nanocomposite conjugated with tobramycin against antibiotic resistant Pseudomonas aeruginosa. *Arabian Journal of Chemistry*, *17*(1), 105458. https://doi.org/10.1016/j.arabjc.2023.105458
32. Yao, C., Yang, S., Shieh, M., & Young, T. (2025). Development of a Chitosan-Silver Nanocomposite/β-1,3-Glucan/Hyaluronic Acid Composite as an Antimicrobial System for Wound Healing. *Polymers*, *17*(3), 350. https://doi.org/10.3390/polym17030350.
33. Zaidi, A. A., Khosa, R., Atiq, A., Usman, M., &Ikhioya, L. I. (2023). Synthesis and Characterization of Chitosan-Silver Nanocomposite Using Chemical Reduction Method and their Antibacterial Properties. *Journal of Nano and Materials Science Research*, 2(1), 117-122. https://doi.org/10.20221/jnmsr.v2i1.17.
34. Zhydzetski, A., Głowacka-Grzyb, Z., Bukowski, M., Żądło, T., Bonar, E., &Władyka, B. (2024). Agents targeting the bacterial cell wall as tools to combat Gram-Positive pathogens. *Molecules*, *29*(17), 4065. https://doi.org/10.3390/molecules29174065.

How to Cite This Article

Sumaila A., Yahaya, M.K., Ibrahim, J., Abdulazeez, M.A., Ibrahim, A., Apeh, K.A., Attah, F., & Peter B.B. (2026). Development and Antimicrobial Performance of Chitosan-Silver Nanocomposites as Sustainable Biomaterials for Building Technology Applications. *NABDA Journal of Biotechnology Research*, 5(2), 57-67.